2834–2844 *Nucleic Acids Research, 2011, Vol. 39, No. 7* *Published online 3 December 2010*
doi:10.1093/nar/gkq1188

Evolution of eukaryal tRNA-guanine transglycosylase: insight gained from the heterocyclic substrate recognition by the wild-type and mutant human and *Escherichia coli* tRNA-guanine transglycosylases

Yi-Chen Chen, Allen F. Brooks, DeeAnne M. Goodenough-Lashua, Jeffrey D. Kittendorf, Hollis D. Showalter and George A. Garcia*

Department of Medicinal Chemistry, College of Pharmacy, University of Michigan, Ann Arbor, MI 48109-1065, USA

Received October 20, 2010; Revised November 3, 2010; Accepted November 4, 2010

ABSTRACT

The enzyme tRNA-guanine transglycosylase (TGT) is involved in the queuosine modification of tRNAs in eukarya and eubacteria and in the archaeosine modification of tRNAs in archaea. However, the different classes of TGTs utilize different heterocyclic substrates (and tRNA in the case of archaea). Based on the X-ray structural analyses, an earlier study [Stengl *et al.* (2005) Mechanism and substrate specificity of tRNA-guanine transglycosylases (TGTs): tRNA-modifying enzymes from the three different kingdoms of life share a common catalytic mechanism. *Chembiochem*, 6, 1926–1939] has made a compelling case for the divergent evolution of the eubacterial and archaeal TGTs. The X-ray structure of the eukaryal class of TGTs is not known. We performed sequence homology and phylogenetic analyses, and carried out enzyme kinetics studies with the wild-type and mutant TGTs from *Escherichia coli* and human using various heterocyclic substrates that we synthesized. Observations with the Cys145Val (*E. coli*) and the corresponding Val161Cys (human) TGTs are consistent with the idea that the Cys145 evolved in eubacterial TGTs to recognize $preQ_1$ but not queuine, whereas the eukaryal equivalent, Val161, evolved for increased recognition of queuine and a concomitantly decreased recognition of $preQ_1$. Both the phylogenetic and kinetic analyses support the conclusion that all TGTs have divergently evolved to specifically recognize their cognate heterocyclic substrates.

INTRODUCTION

Transfer RNA-guanine transglycosylase (TGT, EC 2.4.2.29) is the key enzyme responsible for the queuine [7-((4, 5-cis-dihydroxy-2-cyclopenten-1-yl) amino] methyl-7-deazaguanine (Scheme 1) modification of tRNA in eukarya and eubacteria and archaeosine in archaea (1). In eukarya and eubacteria, TGT incorporates queuine or $preQ_1$ (7-aminomethyl-7-deazaguanine; Scheme 1), respectively, into the anticodon wobble position (position 34) of tRNAs (2,3), while archaeal TGT places another 7-deazaguanine analog, $preQ_0$ (7-cyano-7-deazaguanine), into the position 15 (D loop) of tRNAs (4).

The TGT reaction shares a common mechanism through the replacement of a genetically encoded guanine, shown for the eubacterial TGT to occur via a covalent TGT–RNA intermediate with ping-pong kinetics (5–7). Also, crystallographic evidence reveals that the N-terminal domains of eubacterial and archaeal TGTs fold into an $(\beta/\alpha)_8$ TIM barrel, while a characteristic zinc-binding motif is found in their C-terminal domains (8,9). Romier *et al.* (8) observed a dimer interface when the structure of the *Zymomonas mobilis* TGT was determined. Later, co-crystallization of the enzyme with

*To whom correspondence should be addressed. Tel: +1 734 764 2202; Fax: +1 734 647 8430; Email: gagarcia@umich.edu
Present addresses:
DeeAnne M. Goodenough-Lashua, Department of Chemistry and Biochemistry, University of Notre Dame, Notre Dame, IN 46556-5670, USA.
Jeffrey D. Kittendorf, Alluvium Biosciences, Ann Arbor, MI, USA.

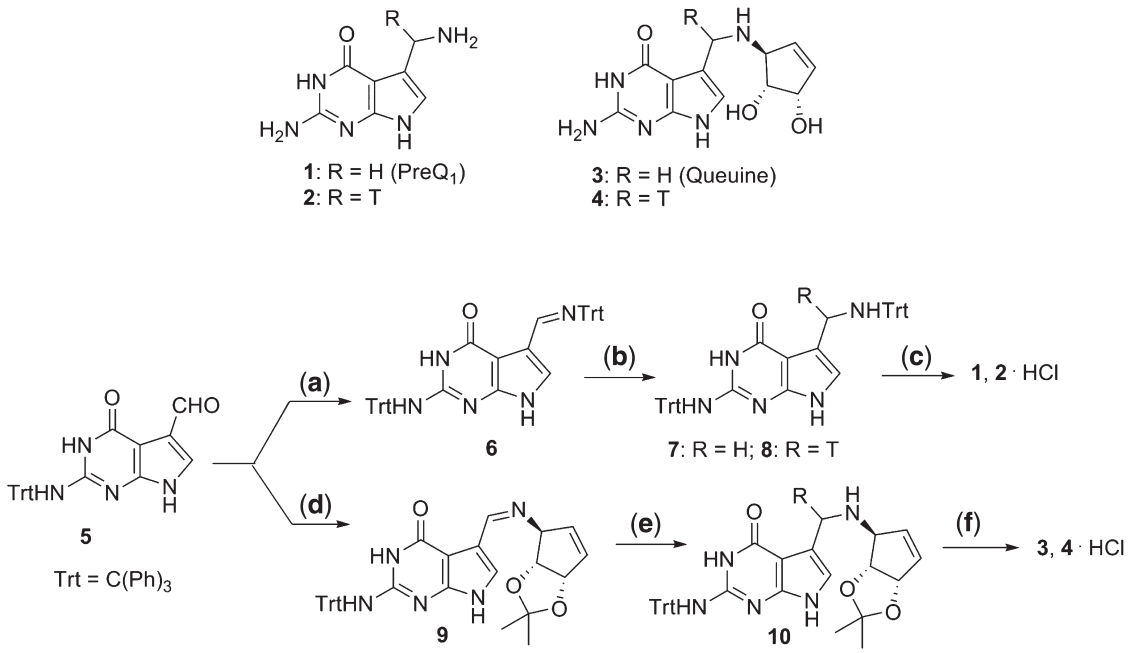

Scheme 1. Synthesis of ^{1}H- and ^{3}H-labeled $PreQ_1$ and Queuine: (**a**) trityl amine, Na_2SO_4, anhydrous THF, reflux, 6 h; (**b**) 2eq. $NaBH_4$ or NaB^3H_4, THF, 0–25°C, 3 h, 79% two steps; (**c**) 1.25 M methanolic HCl, reflux, 2 h, 89%; (**d**) (3*S*,4*R*,5*S*)-3-amino-4,5-isopropylidenedioxy-cyclopentene, Na_2SO_4, MeOH, 25°C, 6 h (32); (**e**) 2eq. $NaBH_4$ or NaB^3H_4, MeOH, 0–25°C, 4 h, 99% two steps (32); (**f**) 1.25 M methanolic HCl, 25°C, 2.5 h, 87% (32).

an anticodon stem–loop confirmed a homodimer formation upon tRNA binding (10). The archaeal TGT has also been shown to contain two monomers per asymmetric unit and the two subunits were suggested to interact tightly through the zinc-binding domain (9). The most interesting subunit structure was found in eukarya. Although lacking a crystal structure, the eukaryal TGT has been proposed for almost four decades to be a heterodimer (11) based upon biochemical and kinetic characterizations. Although there have been discrepancies regarding the reported size and composition of the subunits (11–14), it is now clear that the eukaryal TGT is composed of queuine tRNA-ribosyltransferase (QTRT1) and QTRT domain-containing 1 (QTRTD1), which are homologous subunits of 44 and 46.7 kDa, respectively (15,16). QTRTD1 has been proposed to be the queuine salvage enzyme that liberates free queuine from QMP (16).

An argument has been made that queuosine modification in eubacteria and eukarya may have resulted from convergent evolution based on the dramatic differences between their queuosine modification systems (e.g. eukarya do not synthesize queuine while eubacteria do, and eukarya transport and salvage queuine while eubacteria do not) (17). At that time, the quaternary structure of the eukaryal TGT was thought to be different from that of the eubacterial TGT, as described above. Subsequently, based upon careful analyses of the X-ray crystal structures of eubacterial and archaeal TGTs, Klebe *et al.* (18) have presented a compelling case for the divergent evolution of TGT. Their evidence includes the close overall structural homology and the absolute conservation of zinc-binding and key active-site residues. They also present a cogent discussion of changes in key amino acids in the active site that are responsible for the differential heterocyclic substrate recognition between the eubacterial ($preQ_1$) and archaeal ($preQ_0$) TGTs. However, in the absence of an X-ray crystal structure and any detailed biochemical evidence, extension of the divergent evolution concept to the eukaryal TGT could only be inferred from sequence homologies.

To confirm the divergent evolution model for TGT, we report further sequence homology and phylogenetic analyses, the results of which are consistent with divergent evolution. To provide experimental evidence for the divergent evolution of TGT in eukaryotes, queuine and $preQ_1$ incorporation studies were performed with wild-type and mutant human and *Escherichia coli* tRNA-guanine transglycosylases. Enzymological studies of mutants of Cys145 (*E. coli* TGT) and the corresponding Val161 (human TGT) are consistent with the concept that this residue, in particular, has evolved to enhance recognition of $preQ_1$ in eubacteria and to decrease recognition of $preQ_1$, concomitant with increased recognition of queuine, in eukarya. These phylogenetic analyses and experimental results support the conclusion that all TGTs have divergently evolved to specifically recognize their cognate heterocyclic substrates, while minimizing recognition of non-cognate ones.

MATERIALS AND METHODS

Reagents

Unless otherwise specified, all reagents were ordered from Sigma-Aldrich. DNA oligonucleotides, agarose, dithiothreitol (DTT) and DNA ladders were ordered

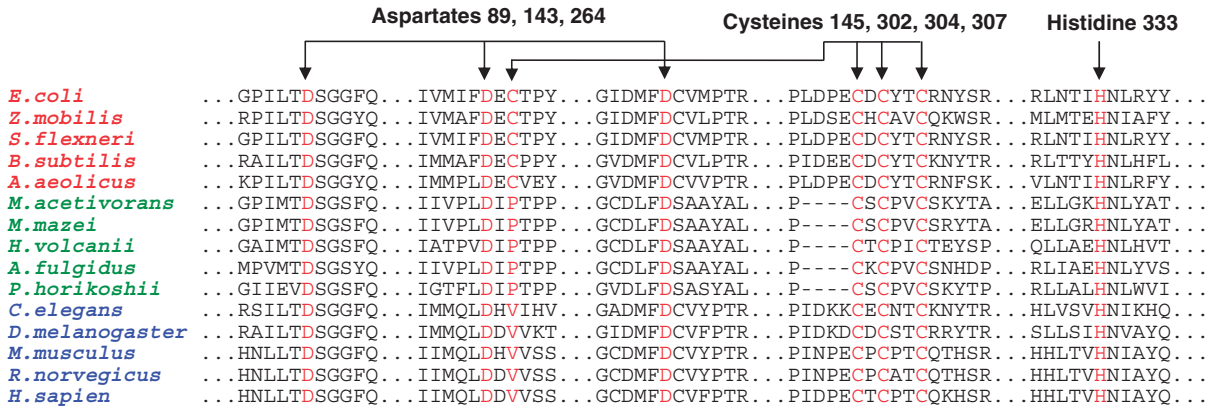

Figure 1. Selected regions of a sequence homology analysis of TGTs across the three kingdoms of life. A sequence alignment of representative TGTs from eubacteria, archaea and eukarya highlighting the conservation of aspartates 89, 143 and 264; cysteines 145, 302, 304 and 307; and histidine 333 (*E. coli* numbering). Dots indicate regions intentionally deleted for this figure. Dashes indicate gaps in the sequence alignment. The full alignment (see Supplementary Figure S17) was generated using PileUP in the SeqWeb software package (Accelerys). The conserved amino acids are colored-coded red.

from Invitrogen. The human $tRNA^{Tyr}$ gene was synthesized by The Midland Certified Reagent Company. All restriction enzymes and Vent® DNA polymerase were ordered from New England Biolabs. The ribonucleic acid triphosphates (NTPs), pyrophosphatase and kanamycin sulfate were ordered from Roche Applied Sciences. The deoxyribonucleic acid triphosphates (dNTPs) were ordered from Promega. Scriptguard™ RNase Inhibitor was ordered from Epicentre. Epicurian coli® XL2-Blue ultracompetent cells were ordered from Agilent Technologies, *E. coli* TG2 and BL21 (DE3) cells were from laboratory stocks. His•Bind resin and lysonase bioprocessing reagent were purchased from Novagen. The QIAPrep® Spin Miniprep and Maxiprep Kits were ordered from Qiagen. Precast PhastGels and SDS buffer strips were from VWR. Bradford reagent was from Bio-Rad. Whatman GF/C Glass Microfibre Filters, Amicon Ultra Centrifugal Filter Devices, carbenicillin and all bacterial media components were ordered from Fisher. [8-^{14}C]-Guanine (50–60 mCi/mmol) was ordered from Moravek Biochemicals and the tritiation of [^{3}H]-preQ$_1$ and [^{3}H]-queuine was also performed by Moravek Biochemicals (see below). T7 RNA polymerase was isolated from *E. coli* BL21 (DE3) pLysS cells harboring the plasmid pRC9 via minor modifications of the procedure described in the literature (19). The human TGT and $tRNA^{Tyr}$ (human and *E. coli*) were generated as previously described (16,20).

Syntheses of [^{3}H]-PreQ$_1$ (2) and [^{3}H]-Queuine (4)

The detailed procedures for these syntheses can be found in the Supplemetary data.

Multiple sequence alignment of representative TGTs across the three kingdoms

The protein sequences of 15 TGTs, spanning the three phylogenic domains, were retrieved using the following accession numbers (*E. coli*, AAA24667; *Z. mobilis*, T46898; *Shigella flexneri*, NP_706294; *Bacillus subtilis*, NP_390649; *Aquifex aeolicus*, NP_213895; *Methanosarcina acetivorans*, NP_619281; *M. mazei*, NP_633125; *Haloferax volcanii*, BAB40327; *Archeoglobus. fulgidus*, NP_070314; *Pyrococcus horikoshii*, NP_143020; *Caenorhabditis elegans*, NP_502268; *Drosophila melanogaster*, NP_608585; *Mus musculus*, NP_068688; *Rattus norvegicus*, NP_071586; *Homosapien*, AAG60033). Sequence alignment was performed using the PileUP alignment program found in the SeqWeb software package (Accelrys). Selected regions highlighting the conservation of aspartates 89, 143 and 264; cysteines 145, 302, 304 and 307; and histidine 333 (*E. coli* numbering) are shown in Figure 1. The full alignment can be found in Supplemetary Figure S12.

Phylogenetic tree for TGTs across the three kingdoms

Amino acid sequences for eubacterial and archaeal TGT and eukaryal QTRT1 and QTRTD1 were manually extracted from the NCBI protein sequence database. A very large number of sequences (approximately 6000) were initially found. In the case of archaeal TGTs, these were sorted by phylogenetic tree and duplicates were discarded. Where a number of examples were present within each subgroup, only 1–2 were selected for inclusion in our study as we wanted the sample to be a diverse representation and not to be biased towards any one subgroup. A large number of protein sequences were annotated as 'PUA domain containing'; however, only those clearly annotated as tRNA transglycosylase or ribosyltransferase (e.g. queuine, guanine, 7-cyano-preQ$_1$ or archaeosine) were included to avoid possible confusion with pseudouridine synthases and others. Due to the large number of subgroups for the eubacterial TGTs, the sequences were sorted by the highest level of identified organisms listed in the database; however, only one example per genus was chosen to minimize bias.

A multiple sequence alignment was then performed with Clustal W. A number of sequences (36) were found to be suspect. Reexamination of the NCBI database allowed us to correct 30 of these sequences. The six sequences that were deleted were found to not align with (or were missing) the conserved active-site aspartates and

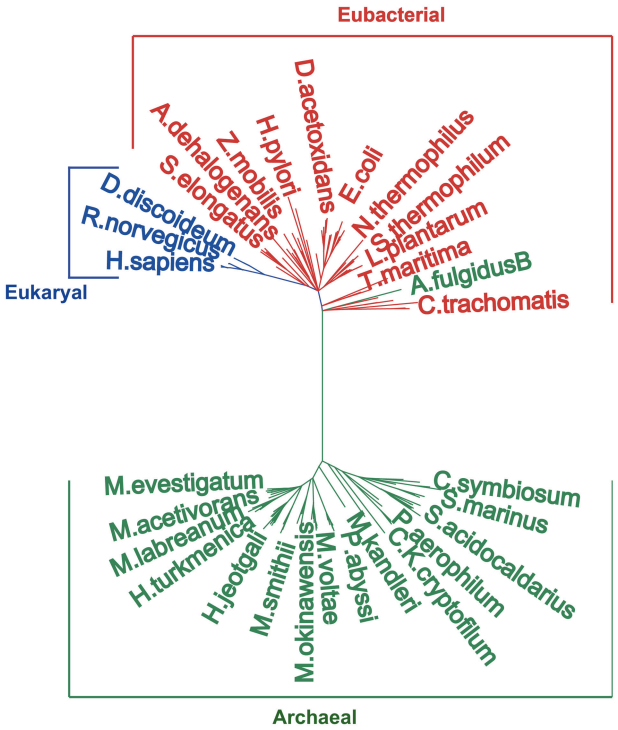

Figure 2. Phylogenetic tree for TGTs across the three Kingdoms. The evolutionary history of the TGT enzymes was inferred via 'maximum likelihood' analysis with the MEGA4 software package. Representative TGT sequences spanning the three domains of life (13 eukaryal, 59 eubacterial and 72 archaeal) were globally aligned using Clustal W. The alignment was subjected to 500 bootstrap replicates resulting in the final consensus phylogenetic tree. This is an unrooted tree and the branch lengths are proportional to the evolutionary distances between nodes. Due to the number of sequences, a condensed version of the tree is shown. The full tree can be seen in Supplementary Figure S13.

zinc-binding ligands (Figure 1) or were of lengths not consistent with the other sequences. This data set contained approximately 100 eubacterial sequences. Our initial tree calculation suggested that the disproportionate number of eubacterial sequences might be biasing the analysis. We therefore pared down the number of eubacterial sequences using the same criterion of maintaining phyogenetic diversity. This yielded 13 eukaryal QTRT1, 72 archaeal TGT and 59 eubacterial TGT sequences. A listing of these sequences can be found in Supplemetary Table S1.

The evolutionary history of the TGT enzymes was then inferred via 'maximum likelihood' analysis using the MEGA4 software package (21,22). The Clustal W alignment was subjected to 500 bootstrap replicates resulting in the final consensus phylogenetic tree. Due to the number of sequences, a condensed version of the tree is shown in Figure 2. The full tree can be seen in Supplemetary Figure S13.

Construction, expression and purification of human TGT and Val161Cys mutant

The wild-type human TGT was prepared as described previously (16). The Val161Cys mutant plasmid was generated by QuikChange™ site-directed mutagenesis (Stratagene) using the wild-type plasmid as a template and the following mutagenic primers: 5′-CATCATCATGCAGCTGGAC GACTGTGTTAGCAGTACTGTGACTGGGCC-3′ and 5′-GGCCCAGTCACAGTACTGCTAACACAGTCGT CCAGCTGCATGATGATG-3′. The Val161Cys mutant was then prepared in the same fashion as the wild-type.

Construction of *E. coli* TGT Cys145 mutants

The Cys145Ala plasmid was previously generated (23) by a combined polymerase chain reaction (PCR)-ligase chain reaction (24). The Cys145Ser plasmid was generated by site-directed mutagenesis using pTGT5 as a template (25) and the following mutagenic primers 5′-GCAGGAT ACGGCGTAGACTCATCAAAGATCATGACG-3′ and 5′-CGTCATGATCTTTGATGAGTCTACGCCGTATC CTGC-3′. The Cys145Asp plasmid was generated as described for Cys145Ser with the following changes: mutagenic primers (5′-GCAGGATACGGCGTGTCTTCAT CAAAGATCATGACG-3′ and 5′-CGTCATGATCTTT GATGAAGACACGCCGTATCCTGC-3′), the total volume of the PCR reaction was 25 µl and the primer concentration was reduced to 0.6 µM. The Cys145Asp PCR product formed DNase sensitive aggregates that were immobile on an agarose gel, and remained after the wild-type plasmid was eliminated by Dpn I digestion. Therefore, the PCR product was diluted 5-fold prior to transformation into competent cells. All resulting plasmids were isolated via Qiagen miniprep, and the *tgt* mutant genes were confirmed by DNA sequencing (University of Michigan DNA Sequencing Core Facilities). To generate the plasmids of polyhistidine-tagged *E. coli* mutants, the *tgt* mutant genes were subcloned into vector pET-28a^{Kan} following general laboratory protocols. The plasmid of polyhistidine-tagged Cys145Val was directly generated using the plasmid of polyhistidine-tagged Cys145Ala as a template and the following mutagenic primers: 5′-CAGTCAGCAGGATACG GCGTAACCTCATCAAAGATCATGACG-3′ and 5′-CGTCATGATCTTTGATGAGGTTACGCCGTATC CTGCTGACTG-3′.

Expression and purification of *E. coli* TGT and Cys145 mutants

The wild-type *E. coli* TGT and Cys145 mutants were prepared following the procedure established by Chong and Garcia (25), with minor modifications. The final enzyme concentrations were determined with the Bio-Rad Protein Assay Kit using BSA as the standard. The proteins were stored in liquid N_2 and utilized to determine guanine and tRNA kinetic parameters. The wild-type polyhistidine-tagged *E. coli* TGT was prepared as described previously (20), and the polyhistidine-tagged *E. coli* TGT mutants were expressed following an auto-induction procedure (26). The final concentration of each protein was determined as described above and the proteins were stored in liquid N_2 and utilized to determine preQ$_1$ kinetic parameters. Note that we have previously determined that the polyhistidine tag has no effect on the TGT reaction or kinetics (27).

Activity screen and kinetic analyses

Heterocyclic base-exchange assays were conducted by monitoring the incorporation of radiolabeled substrates, [8-^{14}C]-guanine, [^{3}H]-preQ$_1$ and [^{3}H]-queuine into either the human or *E. coli* tRNA^{Tyr} using various TGT samples. In brief, kinetic assays were set up under the following conditions: tRNA^{Tyr} (saturating concentrations depending on the K_m for each individual enzyme), individual radiolabeled base (various concentrations), TGT (25, 50 or 100 nM depending on the concentration of heterocyclic base used) and HEPES reaction buffer (100 mM HEPES, pH 7.3; 20 mM $MgCl_2$; 5 mM DTT) to a final volume of 400 µl. The studies were performed in triplicate. All samples were incubated at 37°C for purposes of equilibration before initiating the reaction with the addition of TGT. Aliquots (70 µl) were removed every 2 min throughout the 10-min time course and immediately quenched in 2.5 ml of 5% trichloroacetic acid (TCA) for 1 h before filtering on glass-fiber filters. Each filter was washed with three volumes of 5% TCA and a final wash of ethanol to dry the filter. The samples were analyzed in a scintillation counter (Beckman) for radioactive decay, where counts were reported in DPM and later converted to picomoles [8-^{14}C]-guanine/[^{3}H]-preQ$_1$/[^{3}H]-queuine by following the general conversion between DPM and specific activity (e.g., pmol = DPM × 0.0079, for the [8-^{14}C]-guanine stock with a specific activity of 57 mCi/mmol). To obtain steady-state kinetic parameters, initial velocities of guanine/preQ$_1$/queuine incorporation were determined by converting the slopes of these plots (pmol/min) to units of per second (1/sec), taking into account the concentration of the enzyme and aliquot size. The individual data points from each trial were averaged, and the standard deviation was determined for each concentration of either tRNA^{Tyr} or heterocyclic base. The average data points (with error bars representing their standard deviations) were plotted. However, all of the individual data points were fit via non-linear regression to the Michaelis–Menten equation using KaleidaGraph (Abelbeck Software).

RESULTS

Improved synthesis of PreQ$_1$ (1) and application to preparation of [^{3}H] PreQ$_1$ (2)

In consideration of a suitable synthetic scheme to make [^{3}H]-preQ$_1$ (2), a short, efficient route that could be easily executed with simple reagents was desired. An examination of the literature for the synthesis of cold-labeled compound **1** revealed three previous reports (28–30). The original report of Ohgi *et al.* (28) provides **1** in 6.7% overall yield and requires 12 steps from a non-commercial starting material. A second synthesis by Akimoto *et al.* (29) is much shorter and proceeds via a Mannich reaction to incorporate the aminomethylene side chain of preQ$_1$ regioselectively to the C-5 position of a pyrrolopyrimidine precursor. Its main drawback from a standpoint of radiochemical synthesis is the co-generation of a small amount of C-6 substituted isomer and generally more harsh reaction conditions that would require multiple chromatographic steps following incorporation of label via [^{3}H]-formaldehyde. The recent synthesis of Klepper *et al.* (30) proceeds via readily available preQ$_0$ (31), but the second stage reduction of the nitrile to the aminomethylene group by hydrogenation proceeded only in 10% yield and required tedious purification. Hence, none of these procedures was deemed suitable for our needs. This article reports an exceptionally short, and high yielding synthesis of preQ$_1$ **(1)** from readily available precursors and its utilization in the synthesis of ^{3}H-labeled congener **2**.

Our route is outlined in Scheme 1. Reaction of easily derived aldehyde **5** (32) was examined with a number of ammonia surrogates (benzyl amine, 4-methoxybenzyl amine, 2,4-dimethoxybenzyl amine). While reductive amination proceeded cleanly, subsequent global deprotection under catalytic hydrogenolysis or standard acid conditions did not proceed satisfactorily. Trityl amine was next explored as a surrogate and was found to be ideal. Thus, heating **5** with trityl amine in refluxing THF cleanly formed stable imine **6** in essentially quantitative yield. Reduction of **6** with two equivalents of sodium borohydride then provided **7** in 79% yield following filtration through a plug of silica gel. This was entered directly into a global deprotection with methanolic HCl to provide preQ$_1$ (**1**), which precipiated out of solution as the monohydrochloride salt in 89% yield. The exact same process was then repeated by Moravek Biochemicals using [^{3}H]-sodium borohydride to incorporate the label. The collected product **2** had a specific activity of 7.0 Ci/mmol, and showed chemical and radiochemical purities of 99.5% and 96.1%, respectively, by HPLC (Supplemetary Figures S7 and S8).

Synthesis of [^{3}H]-Queuine (4)

Our route to [^{3}H]-queuine (**4**) is outlined in Scheme 1 and follows directly from our recently published short, high-yielding synthesis of queuine (**3**) (32). The collected product **4** (by Moravek Biochemicals) had a specific activity of 7.3 Ci/mmol and showed chemical and radiochemical purities of 94.1 and 99.4%, respectively, by HPLC (Supplemetary Figures S9–11).

Phylogenetic tree for TGTs across the three kingdoms

A complete search of the NCBI database for TGT sequences and subsequent paring down of some sequences yielded a representative number of sequences that were aligned via Clustal W. This alignment then was used for a phylogenetic tree analysis using MEGA4. The tree analysis (Figure 2) clearly demonstrates the relatedness of the TGT sequences. Consistent with the simple homology analysis, the archaeal sequences clearly group distinctly from the others and the eukaryal sequences group together, but closer to the eubacterial sequences.

Kinetics analysis of human TGT with respect to Queuine and PreQ$_1$

To investigate the heterocyclic substrate specificity of the human TGT (SDS-PAGE in Supplemetary Figure S3A,

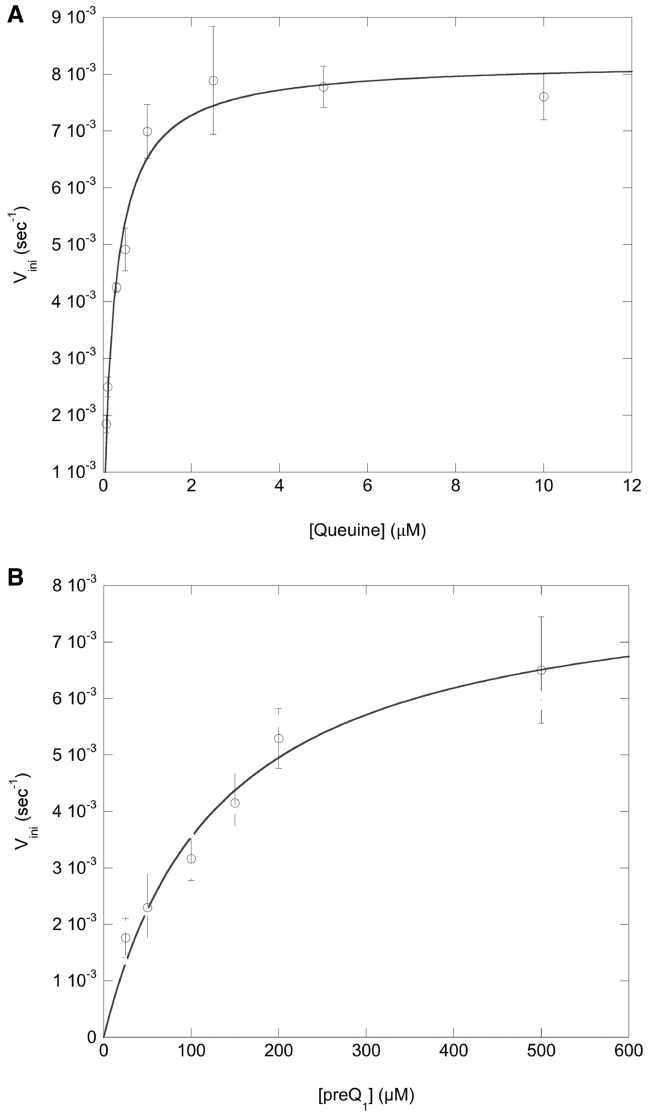

Figure 3. Michaelis–Menten fits of (**A**) Queuine and (**B**) $PreQ_1$ with wild-type human TGT.

lane 2), the transglycosylase activity was measured via monitoring [^{3}H]-queuine and [^{3}H]-$preQ_1$ incorporation into human $tRNA^{Tyr}$. The concentration of tRNA was fixed at saturation (10 μM), as the K_m value was previously determined to be 0.34 ± 0.04 μM (16). The kinetic parameters were then determined by non-linear fits to the Michaelis–Menten equation (Figure 3A and B, Table 1). The results show that the k_{cat} values for both substrates are essentially identical ($\sim 8 \times 10^{-3}\,s^{-1}$); however, the human TGT incorporates its natural heterocyclic substrate, queuine, with a sub-micromolar K_m (0.26 ± 0.03 μM), while a 507-fold larger K_m for $preQ_1$ (132.33 ± 27.61 μM) was observed. Due to the indistinguishable k_{cat} values, the difference in K_m also leads to a significantly higher catalytic efficiency (as defined by k_{cat}/K_m) toward queuine, clearly indicating the preferential recognition of the human TGT for queuine.

Table 1. Kinetic parameters for eukaryotic TGTs with heterocyclic substrates

Enzyme	k_{cat}[a,b] (10^{-3}•s^{-1})	K_m[a,b] (μM)	k_{cat}/K_m[a,b] (10^{-3}•s^{-1}•μM^{-1})
Human			
Queuine	8.22 (0.20)	0.26 (0.03)	31.6 (3.4)
$PreQ_1$	8.23 (0.71)	132 (28)	0.062 (0.014)
Guanine[c]	5.86 (0.10)	0.41 (0.03)	14.2 (0.9)
Rat liver[d]			
Queuine	N.D.[f]	0.29[g]	N.D.
$PreQ_1$	N.D.	2.1[g]	N.D.
Guanine	N.D.	0.83[g]	N.D.
Rabbit Erythrocytes[e]			
Guanine	N.D.	0.15[g]	N.D.

[a]Standard errors are shown in parentheses.
[b]Kinetic parameters were calculated from the average of three replicate determinations of initial velocity data.
[c]Data from Chen *et al.* (16).
[d]Data from Shindo-Okada *et al.* (3).
[e]Data from Howes and Farkas (11).
[f]Not Determined.
[g]No errors reported.

Table 2. $PreQ_1$ kinetics for wild-type and position 145/161 mutant TGTs

Enzyme	k_{cat}[a,b] (10^{-3}•s^{-1})	K_m[a,b] (μM)	k_{cat}/K_m[a,b] (10^{-3}•s^{-1}•μM^{-1})
Escherichia coli			
Wild-type	9.57 (0.24)	0.05 (0.01)	191 (38.6)
Cys145Val	14.1 (0.7)	2.76 (0.5)	5.10 (0.95)
Cys145Ala	74.6 (3.4)	43.4 (5.0)	1.72 (0.21)
Cys145Ser	23.7 (1.0)	123 (13.9)	0.19 (0.02)
Cys145Asp.	N.D.A.[c]	N.D.A.[c]	N.D.A.[c]
Human			
Val161Cys	4.64 (0.32)	22.3 (4.1)	0.21 (0.04)

[a]Standard errors are shown in parentheses.
[b]Kinetic parameters were calculated from the average of three replicate determinations of initial velocity data.
[c]No detectable activity ≤100 μM $preQ_1$.

Kinetics analysis of *E. coli* TGT with respect to Guanine, $PreQ_1$ and Queuine

Similarly, the transglycosylase activity of the *E. coli* TGT (SDS–PAGE in Supplemetary Figure 1, lane 3) was measured via monitoring [8-^{14}C]-guanine, [^{3}H]-$preQ_1$ and [^{3}H]-queuine incorporation into *E. coli* $tRNA^{Tyr}$ (fixed at 10 μM, K_m = 0.19 μM, Table 4). The k_{cat} value for $preQ_1$ was determined to be $9.57 \times 10^{-3}\,s^{-1}$, slightly faster than that of the human enzyme (Table 2 and Figure 4). In addition, the *E. coli* enzyme exhibits a low K_m (~50 nM) for $preQ_1$, suggesting a high affinity in terms of substrate binding. Consistent with the previous report (33), the *E. coli* TGT does not seem to incorporate queuine as a substrate as no detectable transglycosylase activity was observed at queuine concentrations ≤50 μM (data not shown). A low amount of radioactivity (not linear with time) was captured on the filters at higher concentrations of queuine. However, control experiments conducted with no substrate RNA in the reaction mixtures confirm that the background radioactivity most

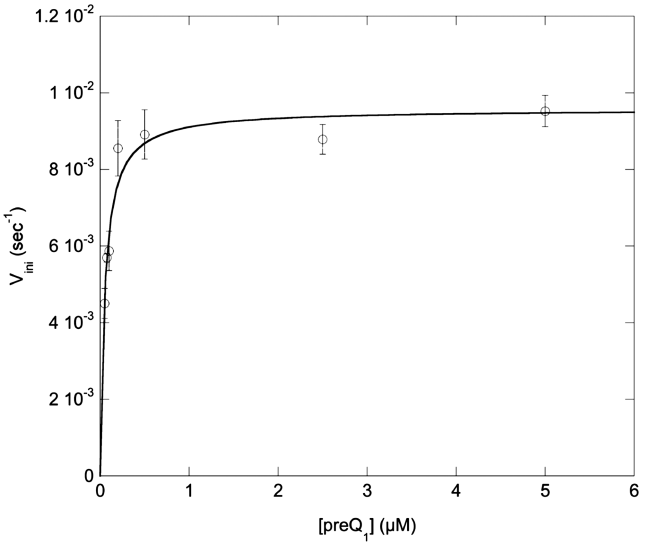

Figure 4. Michaelis–Menten fit of $PreQ_1$ with wild-type *E. coli* TGT.

Table 3. Guanine kinetics for wild-type and Cys145 mutant *E. coli* TGTs

Enzyme	k_{cat}[a,b] (10^{-3}•s^{-1})	K_m[a,b] (μM)	k_{cat}/K_m[a,b] (10^{-3}•s^{-1}•μM^{-1})
Wild-type	6.29 (0.12)	0.35 (0.03)	18.0 (1.6)
Cys145Ala	86.8 (2.1)	2.34 (0.23)	37.1 (3.9)
Cys145Ser	28.0 (0.7)	1.94 (0.17)	14.4 (1.3)
Cys145Asp	5.44 (0.23)	68.1 (7.8)	0.080 (0.01)

[a]Standard errors are shown in parentheses.
[b]Kinetic parameters were calculated from the average of three replicate determinations of initial velocity data.

Table 4. tRNA kinetics for wild-type and Cys145 mutant *E. coli* TGTs

Enzyme	k_{cat}[a,b] (10^{-3}•s^{-1})	K_m[a,b] (μM)	k_{cat}/K_m[a,b] (10^{-3}•s^{-1}•μM^{-1})
Wild-type	5.19 (0.29)	0.19 (0.05)	27.3 (7.3)
Cys145Ala	76.3 (3.1)	1.11 (0.22)	68.7 (14.0)
Cys145Ser	28.2 (1.0)	0.49 (0.09)	58.0 (10.5)
Cys145Asp	6.34 (0.41)	3.30 (0.79)	1.92 (0.48)

[a]Standard Errors are shown in parentheses.
[b]Kinetic parameters were calculated from the average of three replicate determinations of initial velocity data.

likely resulted from either non-specific binding of queuine to the filters (at the higher concentrations) or queuine approaching its limit of solubility, precipitating out of solution and being captured on the filters. The kinetic parameters for guanine and tRNA (Tables 3 and 4) are similar to those previously reported (20).

Kinetics analysis of *E. coli* TGT Cys145 mutants

To confirm the role of active site Cys145 in the *E. coli* TGT, four mutants, Cys145Ala, Cys145Ser, Cys145Asp and Cys145Val (SDS–PAGE in Supplemetary Figure S11A, lanes 4–6 and Figure S11B, lane 2) were generated to probe the heterocyclic substrate recognition using [^{14}C]-guanine and [^{3}H]-$preQ_1$. The kinetic parameters for guanine exchange were determined for both the guanine and tRNA substrates with the alanine, serine and aspartate mutants (Tables 3 and 4; also see Supplemetary Figures S14–16 for the guanine and tRNA kinetic curves). An increase in k_{cat} relative to wild-type is observed for both the Cys145Ala and Cys145Ser mutants (14.5- and 5-fold for Cys145Ala and Cys145Ser, respectively). The activity of the Cys145Asp mutant with guanine is approximately equivalent to that of wild-type TGT. Similar trends in K_m were observed for both substrates with the Cys145Asp and Cys145Ser mutants. Increases, relative to wild-type, in K_m of 6.7- and 5.5-fold were seen with guanine for both enzymes, and 5.8-fold with tRNA for Cys145Ala. The increase in the tRNA K_m relative to wild-type was only slightly less (2.6-fold) with Cys145Ser. However, with the Cys145Asp mutant, the substrate K_ms are very different. While the tRNA K_m increases 17-fold, the guanine K_m is 195-times greater than that of wild-type.

The kinetic parameters for $preQ_1$ exchange were also determined while the concentration of tRNA was maintained at saturating concentration (depending on the tRNA K_m for each individual mutant). Similar to guanine kinetics, an increase in k_{cat} was also observed for both the Cys145Ala and Cys145Ser mutants; however, the differences compared to the wild-type were only 7.8- and 2.5-fold for Cys145Ala and Cys145Ser, respectively (Table 2; also see Supplemetary Figures S17 and S18 for the $preQ_1$ kinetic plots). The enzymatic function of Cys145Asp with respect to $preQ_1$ appears to be abrogated since no activity was found at $preQ_1$ concentrations $\leq$100 μM. Interestingly, the greatest impact on the kinetics comes from the significant increase in K_m for $preQ_1$ with the Cys145Ala and Cys145Ser mutants as the values are 868- and 2460-fold higher than that of the wild-type. The dramatic increase observed in K_m indicates that these two mutants recognize $preQ_1$ much more poorly than the wild-type enzyme. More intriguingly, a valine substitution (which is the corresponding residue in eukarya) at Cys145 only leads to a 55-fold increase in K_m (Table 2 and Supplemetary Figure S19). Furthermore, a human TGT mutant, whose corresponding valine (Val161) was replaced by a cysteine (SDS-PAGE in Supplemetary Figure S11B, lane 3), exhibited a significant improvement in $preQ_1$ recognition (Figure 5) as a substantially lower K_m as well as a higher catalytic efficiency were observed.

DISCUSSION

It has been previously suggested that eubacterial and eukaryal TGTs arose via convergent evolution (17) due to real and perceived differences in the overall pathways for queuine incorporation. More recently a divergent evolution model has been proposed, which is based on careful analyses of the X-ray crystal structures of eubacterial and archaeal TGTs (18). The X-ray crystal structures of

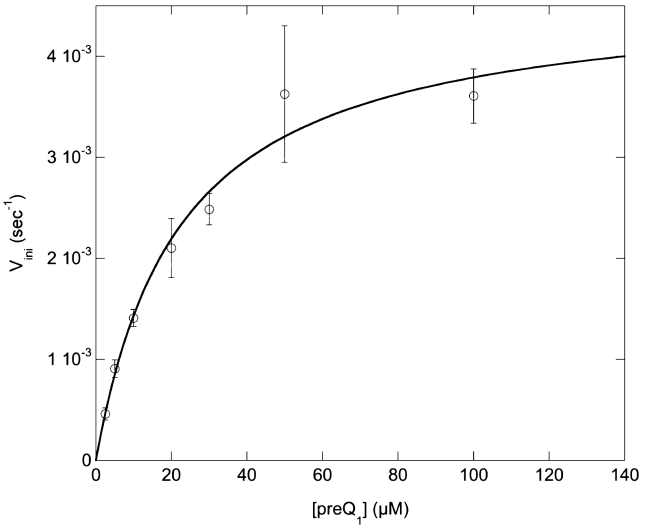

Figure 5. Michaelis–Menten fit of $PreQ_1$ with human TGT Val161Cys.

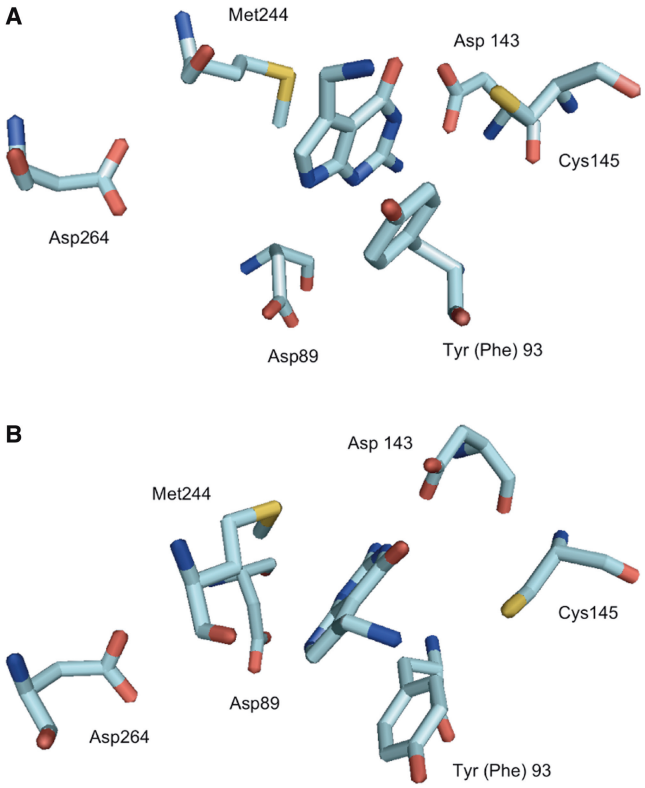

Figure 6. Active site of the $PreQ_1$-bound *Z. mobilis* TGT (PDB accession code 1P0E). The **(A)** and **(B)** (view from two different angles) were generated by PyMOL (The PyMOL Molecular Graphics System, Version 1.3, Schrödinger, LLC). To be consistent with the text, the amino acid residues were labeled based on the *E. coli* numbering. Atoms oxygen, nitrogen and sulfur are highlighted in red, blue and yellow, respectively. Note: Tyr 93 in the *Z. mobilis* TGT corresponds to Phe 93 in the *E. coli* enzyme.

eubacterial and archaeal TGTs (8,9) reveal a common 3D structure including absolute conservation of a structural zinc domain (34). Sequence homologies (Figure 1) in TGTs across the three kingdoms reveal the absolute conservation of the four zinc-binding ligands and three key catalytic aspartates in the active site (Figure 6). Eukaryotes also have a TGT-homolog (QTRTD1), which contains the zinc-binding domain and is homologous to the TGT family, but does not share the absolute conservation of the active-site aspartates. QTRTD1 has been proposed to be the salvage enzyme that hydrolyzes QMP to generate free queuine (35,36). It seems likely that the differences in active site amino acids may be due to the altered chemical reaction that the salvage enzyme catalyzes. All TGTs across the three kingdoms are thought to share the same chemical and kinetic mechanisms (1). Although there is a kingdom-based difference in TGT quaternary structure, a similar subunit structure of the enzyme has been identified, wherein eubacterial and archaeal TGTs form homodimers (8–10) and the eukaryal TGT is a heterodimer of two homologous subunits (15,16). The high degree of sequence conservation and similar dimeric subunit structures suggest that the eukaryal TGTs will be found to share the same tertiary structure as the eubacterial and archaeal TGTs. In this article we sought to provide experimental evidence for the divergent evolution of the eukaryal TGT.

A simple multiple sequence alignment of representative TGTs across the three kingdoms (Figure 1) reflects the absolute conservation of active-site and zinc-binding residues as well as significant additional sequence identity and homology. The phylogenetic tree analysis (Figure 2) clearly demonstrates the relatedness of the TGT sequences. The archaeal sequences grouping quite distinctly from the others as might be expected due to the presence of an additional domain in archaeal TGTs versus eukaryal and eubacterial TGTs. The proximity of the eukaryal sequences to the eubacterial sequences may be due in part to the low number (13 versus 59 and 72) of eukaryal sequences, which may not be sufficient to reveal a larger separation between the eukaryal and eubacterial branches. The multiple sequence alignment and phylogenetic tree analysis both support divergent evolution of eubacterial and archaeal TGTs (18) and are clearly consistent with the extension of this concept to the eukaryal kingdom.

Kinetic experiments using queuine and $preQ_1$ were performed to investigate the heterocyclic substrate recognition of the human TGT. To the best of our knowledge, this is the first report of the kinetics of the eukaryal TGT with respect to queuine and $preQ_1$ via direct incorporation assays. It is surprising that both k_{cat} and K_m with respect to queuine are not substantially different from those of guanine [$5.86 \pm 0.10 \times 10^{-3}\,s^{-1}$ and $0.41 \pm 0.03\,\mu M$, (16)]. Comparison of the catalytic efficiencies (k_{cat}/K_m) revealed that the human TGT appears to utilize queuine only 2–3 times more efficiently than guanine ($31.6 \pm 3.4 \times 10^{-3}\,s^{-1}\mu M^{-1}$ versus $14.2 \pm 0.9 \times 10^{-3}\,s^{-1}\mu M^{-1}$). Given that queuine is the natural substrate for the human TGT and the fact the physiological concentrations are generally estimated to be in the low nanometer range in various eukaryal tissues [e.g. ~3.6 nM in human milk (37)], a substantially lower K_m and a significantly higher k_{cat}/K_m values would have been expected.

However, the fact that queuine incorporation is irreversible (3) whereas guanine insertion simply regenerates the substrate tRNA suggests that the human TGT may not experience significant selection pressure to improve the specificity for queuine over guanine. The slightly improved binding affinity (or catalytic efficiency) toward queuine is likely sufficient for organisms to efficiently generate Q-tRNA. Moreover, since product release is rate-limiting (5) during catalysis, a significant difference in k_{cat} would not be expected if the effect of queuine (e.g., Q-tRNA versus G-tRNA product) on the tRNA off-rate is minimal. Additionally, a recent report shows that the two subunits of the human TGT co-localize into mitochondria (15), suggesting that *in vivo* transglycosylase activity (and hence the differential activity with guanine versus queuine) might be affected by an association with mitochondria which has yet to be studied.

It should be noted that the kinetic parameters reported here for the human TGT differ (Table 1) from those previously reported by Shindo-Okada *et al.* (3) in 1980 for the TGT isolated from rat liver and from those reported by Howes and Farkas in 1978 for the TGT from rabbit erythrocytes (11). In each of those cases, the methods used by the authors were much less precise and quite different from those reported here, largely due to the state of technology available at that time. For example, the 'wash out' assay used by Shindo-Okada *et al.* is much less accurate than the direct incorporation assay reported herein as the wash out assay looks for small differences in a large number (e.g., observing the loss of pre-exchanged [^{14}C]-guanine from tRNA). In addition, heterogenous tRNA was employed as a substrate by Shindo-Okada *et al.* and only 3–4 concentrations of the heterocyclic substrate were used to establish kinetic parameters. Furthermore, those assays employed single time points (2 h), with no assurance that the reaction was linear out to this endpoint. Finally, a considerable amount of error is introduced by fitting the data to a linear, double reciprocal plot versus the non-linear fit directly to the Michaelis–Menten equation that was used in the present report.

The 510-fold lower k_{cat}/K_m for preQ$_1$, relative to queuine, with the human TGT indicates that the enzyme preferentially utilizes queuine. This observation nicely matches the homology modeling results of the eukaryal TGT, as the two hydroxyls on the cyclopentenediol moiety are predicted to be capable of forming hydrogen bonds with the enzyme active site residues (34). If one assumes that changes in K_m correlate well with changes in K_D, a 507-fold increase in K_m in this case would represent close to 4 kcal/mol difference in binding free energy [as estimated by $\Delta(\Delta G) = -RT\Delta(\ln K)$]. This could reasonably account for the gain in binding free energy provided by additional hydrogen bonds. On the other hand, the *E. coli* TGT utilizes preQ$_1$ with a high affinity (K_m = 50 nM) as expected, but does not recognize queuine at all as the cyclopentenediol moiety appears to be too bulky to be accommodated by the enzyme (34).

To further examine heterocyclic substrate recognition, a series of cysteine 145 mutants was generated to investigate the role of this residue in the *E. coli* TGT. Although previous work has suggested a hydrophobic interaction between this residue and the 7-aminomethyl moiety of the base (8,34), there has been no kinetic evidence to support this interaction. To probe this, the alanine mutant at this position was generated and expected to display an attenuated hydrophobic effect due to the smaller side chain. In contrast, serine is slightly smaller in comparison to cysteine, but more polar because of the large electronegativity of the oxygen while a negatively charged aspartic acid (at physiological pH) would likely be involved in strong electrostatic interactions.

A few significant observations arose from the kinetic characterization of the Cys145 mutants. First, the parallel increases in K_m values for both the guanine and tRNA substrates (Tables 3 and 4) suggest that similar interactions occur between this residue and guanine whether the base is free or integrated within the tRNA macromolecule. Second, comparing the k_{cat}/K_m values for the enzymes with respect to preQ$_1$ (Table 2), the expected trend, wild-type > Cys145Val > Cys145Ala > Cys145Ser > Cys145Asp (not actually detected) was observed, in accordance with the crystallographic evidence that Cys145 interacts with the base via a hydrophobic interaction as either polar or charged amino acid substitutions lead to a decrease or even loss of substrate recognition. These data are consistent with the concept that the *E. coli* TGT has evolved the nature of the amino acid at position 145 to optimize recognition of preQ$_1$. Moreover, the k_{cat}/K_m value for preQ$_1$ with the human TGT Val161Cys mutant (Table 2) is 3.4-fold higher than that with the wild-type human enzyme. Val161 of the human TGT corresponds to Cys145 in the *E. coli* TGT, therefore this increase catalytic efficiency with respect to preQ$_1$ supports the concept that TGTs have divergently evolved the amino acid at this position to specifically recognize the cognate substrate (e.g. preQ$_1$ versus queuine).

In the case of guanine, the trend in k_{cat}/K_m is slightly different (Cys145Ala > wild-type > Cys145Ser > Cys145Asp) and the reason for this difference is not obvious. The significant increase in k_{cat} for the alanine and serine mutants indicate that the off-rate for the product tRNA has increased and suggests that the substrate tRNA might exhibit a higher K_m. This is true for the alanine mutant, but not for the serine mutant. The serine mutant has a k_{cat}/K_m that is very similar to that for the wild-type. Both k_{cat} and K_m are increased by factors of 4.5 and 5.5, again consistent with faster off rates of product tRNA and substrate guanine; however, substrate tRNA exhibits a K_m only 2.6-fold higher than that for the wild-type TGT. It is possible that there might be a water molecule mediating the interactions between the side chain of Cys145Ser and guanine. In support of this hypothesis, Klebe and co-workers have found a crystallographically well-defined water molecule mediating a hydrogen bond between imidazole ligands (which they extrapolate to the N^7 of G$_{34}$ of the substrate tRNA) and the peptide backbone in the active site (18).

The pK_a of the aminomethyl side chain of preQ$_1$ has been previously determined to be 9.8 in solution (38) and therefore, preQ$_1$ will be protonated at physiological pH,

enabling it to participate in a possible electrostatic interaction with active site residues (Figure 6). However, the severely reduced recognition of $preQ_1$ by the aspartate mutant clearly rejects an electrostatic interaction with the residue at 145. Crystallographic evidence has shown that the amino group of the $preQ_1$ side chain forms a hydrogen bond with the carboxyl oxygen of Leu215 (*E. coli* numbering) (34). A hydrogen bond with the protonated $preQ_1$ side chain would provide a substantial contribution (greater than a simple, non-charged hydrogen bond) to the binding free energy. Another interesting fact is that both the serine and alanine mutants exhibited an increase in k_{cat}. The TGT-catalyzed reaction is extremely slow (approximately one turnover every 2 minutes). Thus, the increases in activity exhibited by those two mutants are significant. However, this observation is not surprising considering product release is rate-limiting (5). Since Cys145 directly interacts with the base, removal of this interaction would enable faster product release. In sum, these observations are consistent with the postulate that Cys145 evolved in eubacteria to selectively recognize $preQ_1$.

The fact that the eubacterial and eukaryal TGTs selectively recognize their cognate heterocyclic substrates is evolutionarily significant. Unlike eubacteria, which biosynthesize queuine from its precursor $preQ_1$, eukarya lack a queuine biosynthesis pathway and are required to obtain queuine from diet as a nutrient factor (39) or through a salvage mechanism that is yet to be fully characterized (40). In addition, while absent in eubacteria, a specific transport system responsible for the cellular uptake of queuine was observed in human fibroblasts and the process appears to be modulated by protein kinase C (PKC) phosphorylation (41,42). We conclude that these differences are most likely due to an outcome of evolution, while the origin of eukarya somehow lost the ability to produce Q-tRNA from $preQ_1$-tRNA. Since the incorporation of $preQ_1$ would not lead to the generation of Q-tRNA, it is likely that due to selection pressure, the eukaryal TGT evolved to take up queuine directly in order to compensate for the inability to synthesize queuine *de novo*. It is also an interesting note that there is a 6-fold difference in k_{cat}/K_m between the human and *E. coli* TGTs with respect to their cognate substrates (Tables 1 and 2). Considering eubacteria need to complete the queuosine biosynthesis pathway to obtain Q-tRNA while eukarya do not, the greater efficiency of the eubacterial TGT seems perfectly plausible.

In conclusion, all of the data generated in this study suggest that the present classes of TGT have arisen via divergent, not convergent, evolution. Future studies are planned in which we are attempting to confirm the postulate that QTRTD1 is the queuine salvage enzyme (mentioned in the 'Introduction'). Consistent with the conclusions herein, it is intriguing to speculate, and consistent with the conclusions of this article, that in eukaryotes, TGT evolved into the queuine-specific transglycosylase and into the salvage enzyme that helps to provide free queuine for the transglycosylase.

SUPPLEMENTARY DATA

Supplementary data are available at NAR online.

ACKNOWLEDGEMENTS

The authors thank Stefanie V. Stachura and Dr. Julie K. Hurt for preparing the constructs of polyhistidine-tagged *E. coli* TGT mutants. They also wish to acknowledge Moravek Biochemicals for conducting the tritiation for the [^{3}H]-$preQ_1$ and [^{3}H]-queuine syntheses.

FUNDING

University of Michigan, College of Pharmacy, Vahlteich and UpJohn Research funds (to G.A.G. and to H.D.H.S.). The open access publication charge for this paper has been partially waived by Oxford University Press - *NAR* Editorial Board members are entitled to one free paper per year in recognition of their work on behalf of the journal.

Conflict of interest statement. None declared.

REFERENCES

1. Garcia,G.A. and Kittendorf,J.D. (2005) Transglycosylation: A mechanism for RNA modification (and editing?). *Bioorg. Chem.*, **33**, 229–251.
2. Okada,N. and Nishimura,S. (1979) Isolation and characterization of a guanine insertion enzyme, a specific tRNA transglycosylase, from *Escherichia coli*. *J. Biol. Chem.*, **254**, 3061–3066.
3. Shindo-Okada,N., Okada,N., Ohgi,T., Goto,T. and Nishimura,S. (1980) Transfer ribonucleic acid guanine transglycosylase isolated from rat liver. *Biochemistry*, **19**, 395–400.
4. Watanabe,M., Matsuo,M., Tanaka,S., Akimoto,H., Asahi,S., Nishimura,S., Katze,J.R., Hashizume,T., Crain,P.F., McCloskey,J.A. *et al.* (1997) Biosynthesis of archaeosine, a novel derivative of 7-deazaguanosine specific to archaeal tRNA, proceeds *via* a pathway involving base replacement on the tRNA polynucleotide chain. *J. Biol. Chem.*, **272**, 20146–20151.
5. Garcia,G.A., Chervin,S.M. and Kittendorf,J.D. (2009) Identification of the rate-determining step of tRNA-guanine transglycosylase from *Escherichia coli*. *Biochemistry*, **48**, 11243–11251.
6. Goodenough-Lashua,D.M. and Garcia,G.A. (2003) tRNA-Guanine transglycosylase from *Escherichia coli*: a ping-pong kinetic mechanism is consistent with nucleophilic catalysis. *Bioorg. Chem.*, **31**, 331–344.
7. Xie,W., Liu,X.J. and Huang,R.H. (2003) Chemical trapping and crystal structure of a catalytic tRNA guanine transglycosylase covalent intermediate. *Nat. Struct. Biol.*, **10**, 781–788.
8. Romier,C., Reuter,K., Suck,D. and Ficner,R. (1996) Crystal structure of tRNA-guanine transglycosylase: RNA modification by base exchange. *EMBO J.*, **15**, 2850–2857.
9. Ishitani,R., Nureki,O., Fukai,S., Kijimoto,T., Nameki,N., Watanabe,M., Kondo,H., Sekine,M., Okada,N., Nishimura,S. *et al.* (2002) Crystal structure of archaeosine tRNA-guanine transglycosylase. *J. Mol. Biol.*, **318**, 665–677.
10. Stengl,B., Meyer,E.A., Heine,A., Brenk,R., Diederich,F. and Klebe,G. (2007) Crystal structures of tRNA-guanine transglycosylase (TGT) in complex with novel and potent inhibitors unravel pronounced induced-fit adaptations and suggest dimer formation upon substrate binding. *J. Mol. Biol.*, **370**, 492–511.
11. Howes,N.K. and Farkas,W.R. (1978) Studies with a homogeneous enzyme from rabbit erythrocytes catalyzing the insertion of guanine into tRNA. *J. Biol. Chem.*, **253**, 9082–9087.

12. Walden,T.L. Jr, Howes,N. and Farkas,W.R. (1982) Purification and properties of guanine, queuine-tRNA transglycosylase from wheat germ. *J. Biol. Chem.*, **257**, 13218–13222.
13. Morris,R.C., Brooks,B.J., Eriotou,P., Kelly,D.F., Sagar,S., Hart,K.L. and Elliott,M.S. (1995) Activation of transfer RNA-guanine ribosyltransferase by protein kinase C. *Nucleic Acids Res.*, **23**, 2492–2498.
14. Slany,R.K. and Mueller,S.O. (1995) tRNA-guanine transglycosylase from bovine liver - Purification of the enzyme to homogeneity and biochemical characterization. *Eur. J. Biochem.*, **230**, 221–228.
15. Boland,C., Hayes,P., Santa-Maria,I., Nishimura,S. and Kelly,V.P. (2009) Queuosine formation in eukaryotic tRNA occurs via a mitochondria-localized heteromeric transglycosylase. *J. Biol. Chem.*, **284**, 18218–18227.
16. Chen,Y.C., Kelly,V.P., Stachura,S.V. and Garcia,G.A. (2010) Characterization of the human tRNA-guanine transglycosylase: Confirmation of the heterodimeric subunit structure. *RNA*, **16**, 958–968.
17. Morris,R.C. and Elliott,M.S. (2001) Queuosine modification of tRNA: a case for convergent evolution. *Mol. Genet. Metab.*, **74**, 147–159.
18. Stengl,B., Reuter,K. and Klebe,G. (2005) Mechanism and substrate specificity of tRNA-guanine transglycosylases (TGTs): tRNA-modifying enzymes from the three different kingdoms of life share a common catalytic mechanism. *Chembiochem*, **6**, 1926–1939.
19. He,B., Rong,M.Q., Lyakhov,D., Gartenstein,H., Diaz,G., Castagna,R., McAllister,W.T. and Durbin,R.K. (1997) Rapid mutagenesis and purification of phage RNA polymerases. *Protein Expr. Purif.*, **9**, 142–151.
20. Kittendorf,J.D., Barcomb,L.M., Nonekowski,S.T. and Garcia,G.A. (2001) tRNA-guanine transglycosylase from *Escherichia coli*: Molecular mechanism and role of aspartate 89. *Biochemistry*, **40**, 14123–14133.
21. Kumar,S., Nei,M., Dudley,J. and Tamura,K. (2008) MEGA: a biologist-centric software for evolutionary analysis of DNA and protein sequences. *Brief. Bioinform.*, **9**, 299–306.
22. Tamura,K., Dudley,J., Nei,M. and Kumar,S. (2007) MEGA4: molecular evolutionary genetics analysis (MEGA) software version 4.0. *Mol. Biol. Evol.*, **24**, 1596–1599.
23. Chong,S., Curnow,A.W., Huston,T.J. and Garcia,G.A. (1995) tRNA-guanine transglycosylase from *Escherichia coli* is a zinc metalloprotein. Site-directed mutagenesis studies to identify the zinc ligands. *Biochemistry*, **34**, 3694–3701.
24. Michael,S.F. (1994) Mutagenesis by incorporation of a phosphorylated oligo during PCR amplification. *BioTechniques*, **16**, 410–412.
25. Chong,S. and Garcia,G.A. (1994) A versatile and general prokaryotic expression vector, pLACT7. *BioTechniques*, **17**, 686–691.
26. Studier,F.W. (2005) Protein production by auto-induction in high density shaking cultures. *Protein Expression Purif.*, **41**, 207–234.
27. Todorov,K.A. and Garcia,G.A. (2006) Role of aspartate 143 in *Escherichia coli* tRNA-guanine transglycosylase: alteration of heterocyclic substrate specificity. *Biochemistry*, **45**, 617–625.
28. Ohgi,T., Kondo,T. and Goto,T. (1979) Synthesis of 7-aminomethyl-7-deazaguanine, one of the nucleoside Q (queuosine) precursors for the post-transcriptional modification of tRNA. *Chem. Lett.*, 1283–1286.
29. Akimoto,H., Imamiya,E., Hitaka,T., Nomura,H. and Nishimura,S. (1988) Synthesis of queuine, the base of naturally occuring hypermodified nucleoside (queuosine), and its analogues. *J. Chem. Soc., Perkin Trans.*, **1**, 1638–1644.
30. Klepper,F., Polborn,K. and Carell,T. (2005) Robust synthesis and crystal-structure analysis of 7-cyano-7-deazaguanine (PreQ(0) base) and 7-(aminomethyl)-7-deazaguanine (PreQ(1) base). *Helv. Chim. Acta.*, **88**, 2610–2616.
31. Migawa,M.T., Hinkley,J.M., Hoops,G.C. and Townsend,L.B. (1996) A two step synthesis of the nucleoside Q precursor 2-amino-5-cyanopyrrolo[2,3-*d*]pyrimidin-4-one ($PreQ_0$). *Synth. Commun.*, **26**, 3317–3322.
32. Brooks,A.F., Garcia,G.A. and Showalter,H.D. (2010) A short, concise synthesis of queuine. *Tetrahedron Lett.*, **51**, 4163–4165.
33. Okada,N., Noguchi,S., Nishimura,S., Ohgi,T., Goto,T., Crain,P.F. and McCloskey,J.A. (1978) Structure determination of a nucleoside Q precursor isolated from *E. coli* tRNA: 7-(aminomethyl)-7-deazaguanine. *Nucleic Acids Res.*, **5**, 2289–2296.
34. Romier,C., Meyer,J.E.W. and Suck,D. (1997) Slight sequence variations of a common fold explain the substrate specificities of tRNA-guanine transglycosylases from the three kingdoms. *FEBS Lett.*, **416**, 93–98.
35. Gunduz,U. and Katze,J.R. (1984) Queuine salvage in mammalian-cells - Evidence that queuine is generated from queuosine 5′-phosphate. *J. Biol. Chem.*, **259**, 1110–1113.
36. Kirtland,G.M., Morris,T.D., Moore,P.H., O'Brian,J.J., Edmonds,C.G., McCloskey,J.A. and Katze,J.R. (1988) Novel salvage of queuine from queuosine and absence of queuine synthesis in *Chlorella pyrenoidosa* and *Chlamydomonas reinhardii*. *J. Bacteriol.*, **170**, 5633–5641.
37. Katze,J.R., Basile,B. and McClosky,J.A. (1982) Queuine, a modified base incorporated posttranscriptionally into transfer RNA: Wide distribution in nature. *Science*, **216**, 55–56.
38. Hoops,G.C., Park,J., Garcia,G.A. and Townsend,L.B. (1996) The synthesis and determination of acidic ionization constants of certain 5-substituted 2-aminopyrrolo[2,3-d]pyrimidin-4-ones and methylated analogs. *J. Heterocycl. Chem.*, **33**, 767–781.
39. Farkas,W.R. (1980) Effect of diet on the queuosine family of tRNAs of germ-free mice. *J. Biol. Chem.*, **255**, 6832–6835.
40. Reyniers,J.P., Pleasants,J.R., Wostmann,B.S., Katze,J.R. and Farkas,W.R. (1981) Administration of exogenous queuine is essential for the biosynthesis of the queuosine-containing transfer RNAs in the mouse. *J. Biol. Chem.*, **206**, 11591–11594.
41. Elliott,M.S., Katze,J.R. and Trewyn,R.W. (1984) Relationship between a tumor promoter-induced decrease in queuine modification of transfer RNA in normal human cells and the expression of an altered cell phenotype. *Cancer Res.*, **44**, 3215–3219.
42. Morris,R.C., Brooks,B.J., Hart,K.L. and Elliott,M.S. (1996) Modulation of queuine uptake and incorporation into tRNA by protein kinase C and protein phosphatase. *Biochim. Biophys. Acta, Mol. Cell Res.*, **1311**, 124–132.